

Department of Pharmacology  
**Qualifying Examination (Part I)**

December 18 & 19, 2007

Please remember that this is a closed-book examination. You must be prepared to answer 4 of the 7 questions. Although not necessary, you may prepare written answers, overhead figures, or any type of materials that you think might be useful in the presentation of your answers. You may bring such preparation materials with you to the examination. The oral examination itself will not extend beyond two hours.

If you have any questions regarding the examination, please contact Joey Barnett at:

936-1722 (w)  
385-4396 (h)  
300-9569 (c)

**BEST WISHES FOR YOUR SUCCESSFUL COMPLETION OF THE EXAMINATION!**

Hypothalamic peptide hormones regulate the secretion of most of the anterior pituitary hormones including GH, FSH, LH, TSH and ACTH. Although prolactin is an important anterior pituitary hormone involved in pregnancy and lactation, a specific prolactin-releasing hormone remains unknown.

Previous studies in your laboratory have suggested that prolactin release is mediated via an arachidonic acid signaling pathway and you attempt to purify this putative releasing factor using arachidonic acid metabolite release as a functional assay. After HPLC fractionation of hypothalamic extracts and an assay in which column fractions were applied to primary anterior pituitary cultures, you obtained the results shown below:

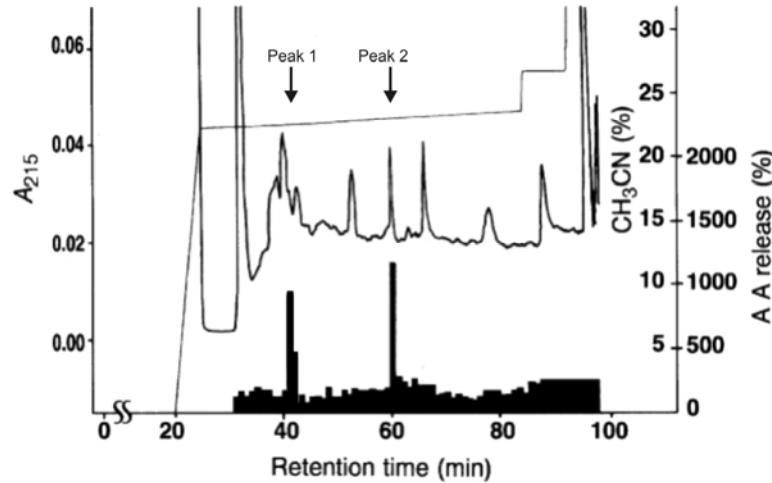


**Figure 1. Reversed-phase (C<sub>18</sub>) HPLC analysis of hypothalamic extracts for AA-releasing activity.** The retention times of multiple peaks with AA-releasing activity are shown along with the protein elution profile (A<sub>215</sub>) and CH<sub>3</sub>CN gradient used for peptide elution.

Concentration-response curves were then performed with the isolated peptides on primary anterior pituitary cultures, yielding the results indicated below:

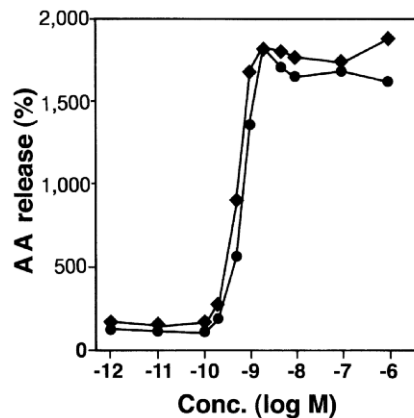


**Figure 2. AA-releasing activity of purified hypothalamic peptides.**

a) Provide at least three plausible explanations for the functional identification of multiple peptides in your assay and detail a series of experiments to determine whether either of these isolated molecules is responsible for the physiological regulation of prolactin release.

b) Assuming that you identify at least one prolactin-releasing peptide (PrRP), outline a strategy for identifying/cloning the receptor through which this peptide ligand acts.

Control of glomerular filtration rate by tubuloglomerular feedback (TGF) involves soluble signals released from macula densa cells that vasoconstrict the afferent arterioles. Recent studies have demonstrated that similar, if not the same, soluble signals cause vasodilation of the efferent arterioles. The leading candidates for mediators of afferent arteriole vasoconstriction are adenosine and ATP. However, which of these signals mediates efferent arteriole vasodilation is not clear.

A Dutch research team investigated the mechanism of efferent arteriolar vasodilation during TGF. For a model system, the investigators used isolated rabbit cortical nephrons in which they perfused the thick ascending limb (TAL) near the macula densa at a constant rate (15 nl/min) with fluids of different NaCl concentration (either 10 or 80 mM) while monitoring efferent arteriolar diameter with videomicroscopy. Because efferent arterioles of isolated nephrons have no basal tone, a low concentration of norepinephrine was applied during experiments to pre-constrict these vessels. The following figures illustrate their experiments.

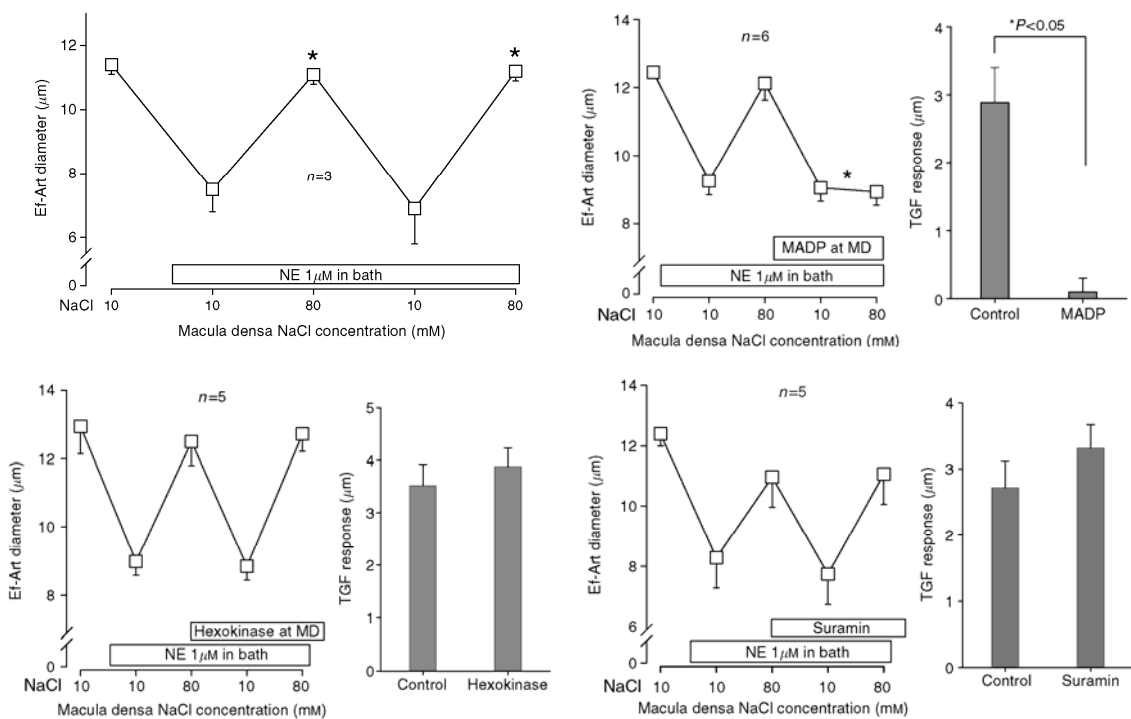


**Fig 1** – Response of efferent arteriolar diameter (y-axis) to changes in TAL/macula densa perfusion (\*,  $p < 0.05$  comparing 80 to 10 mM NaCl). MADP is a competitive inhibitor of 5'-nucleotidase responsible for converting ADP to adenosine. Hexokinase converts ATP to ADP. Suramin is a competitive antagonist of P2X purinergic receptors.

**Questions:**

1. Interpret these data and develop a mechanistic model to explain the response of the efferent arterioles to changes in tubular fluid NaCl concentration.
2. Compare and contrast the mechanism of efferent arteriolar responses to that known for the afferent arteriolar response in TGF.
3. Propose a hypothesis to account for the different behaviors of afferent and efferent arterioles during TGF, and explain how you would test your hypothesis.

**Objective:** To study the disposition of single doses of phenytoin and itraconazole when administered alone and after chronic treatment with the other drug.

**Methods:** Healthy male volunteers were randomized to two groups and studied in parallel. In group 1, a single 200 mg oral dose of itraconazole was administered on two occasions (alone and after 15 days of 300 mg oral phenytoin once daily). Subjects in group 2 were given a single 300 mg oral dose of phenytoin before and after 15 days of itraconazole (200 mg once daily). Blood was collected for 96 hours after each single dose of phenytoin or itraconazole. Serum was assayed for itraconazole and hydroxyitraconazole concentration by HPLC and for phenytoin concentration by fluorescence polarization immunoassay.

[Notes:  
Itraconazole is known to exhibit saturation kinetics.  
Hydroxyitraconazole is an active metabolite of itraconazole.]

Results are shown in the Figures and summarized in the Tables (which show only the mean values +/- SD).

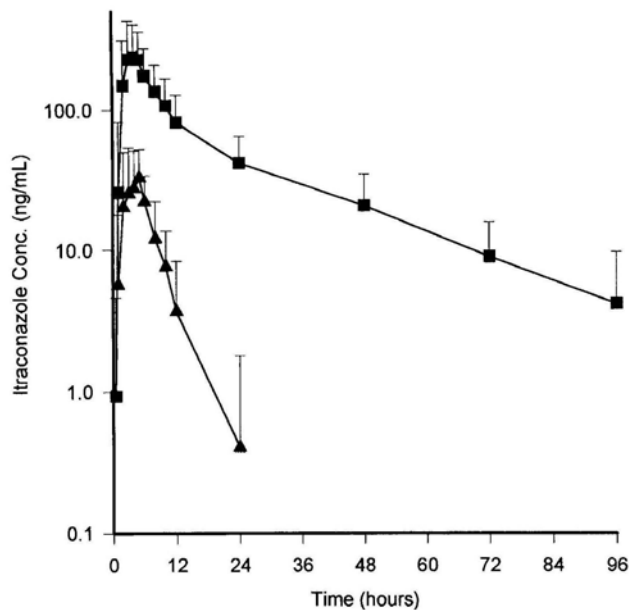


Fig. 1. Mean  $\pm$  SD itraconazole serum concentrations (conc.) versus time after administration of a single 200 mg oral dose during control conditions (solid squares) and after 15 days of treatment with 300 mg oral phenytoin per day (solid triangles).

Mean $\pm$ SD	3203 $\pm$ 1858	224 $\pm$ 190	88.8 $\pm$ 62.1	1318.6 $\pm$ 617.7	215.0 $\pm$ 106.3	36.9 $\pm$ 25.8	22.3 $\pm$ 7.3	3.8 $\pm$ 2.5	—
p Value	—	<0.01	—	<0.01	—	<0.01	—	<0.01	—

AUC, Area under the curve from time zero to infinity; CL/F, oral clearance;  $C_{max}$ , peak concentration;  $t_{1/2}$ , elimination half-life.

in

Mean $\pm$ SD	3203 $\pm$ 1858	224 $\pm$ 190	88.8 $\pm$ 62.1	1318.6 $\pm$ 617.7	215.0 $\pm$ 106.3	36.9 $\pm$ 25.8	22.3 $\pm$ 7.3	3.8 $\pm$ 2.5	—
p Value	—	<0.01	—	<0.01	—	<0.01	—	<0.01	—

AUC, Area under the curve from time zero to infinity; CL/F, oral clearance;  $C_{max}$ , peak concentration;  $t_{1/2}$ , elimination half-life.

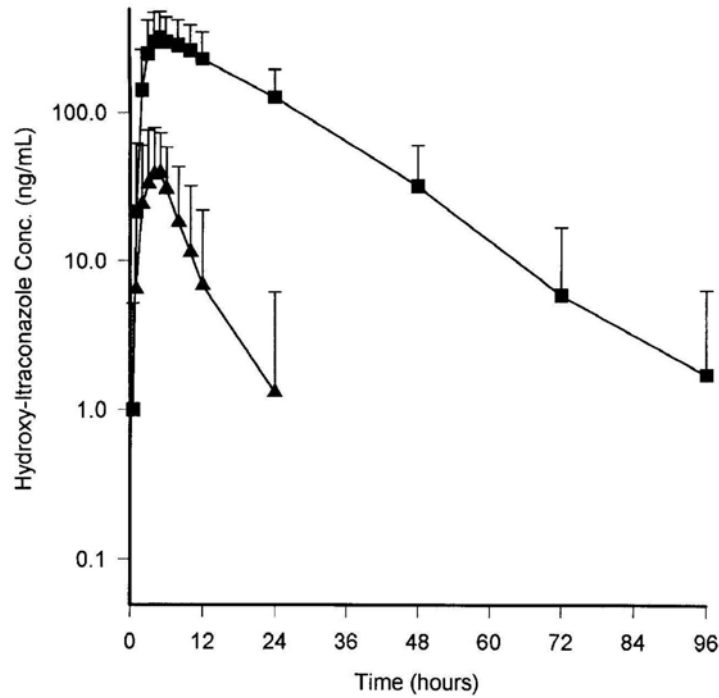


Fig. 2. Mean  $\pm$  SD hydroxyitraconazole serum concentrations (conc.) versus time after administration of a single 200 mg oral dose of itraconazole during control conditions (solid squares) and after 15 days of treatment with 300 mg oral phenytoin per day (solid triangles).

Table II. Pharmacokinetics of hydroxyitraconazole alone and with phenytoin

Subject No.	AUC (ng · hr/ml)		C <sub>max</sub> (ng/ml)		t <sub>1/2</sub> (hr)	
	Control	Phenytoin	Control	Phenytoin	Control	Phenytoin
Mean $\pm$ SD	6224 $\pm$ 3114	315 $\pm$ 447	288.8 $\pm$ 117.9	44.9 $\pm$ 40.5	11.3 $\pm$ 4.2	2.9 $\pm$ 1.4
p Value	—	<0.01	—	<0.01	—	<0.01

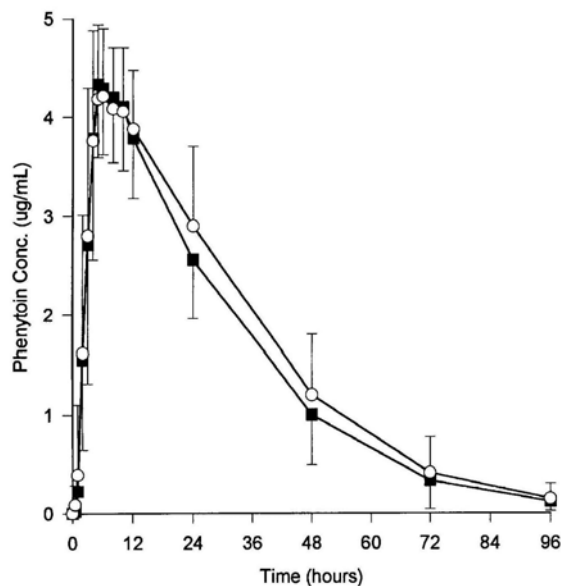


Fig. 3. Mean  $\pm$  SD phenytoin serum concentrations (conc.) versus time after administration of a single 300 mg oral dose of phenytoin during control conditions (solid squares) and after 15 days of treatment with 200 mg oral itraconazole per day (open circles).

Table III. Pharmacokinetics of phenytoin alone and with itraconazole

Parameter	Control	Itraconazole	p Value
AUC ( $\mu\text{g} \cdot \text{hr/ml}$ )	143.8 $\pm$ 39.2	158.7 $\pm$ 50.2	<0.01
C <sub>max</sub> ( $\mu\text{g/ml}$ )	4.6 $\pm$ 0.6	4.6 $\pm$ 0.5	0.9
t <sub>max</sub> (hr)	5.1 $\pm$ 1.4	6.0 $\pm$ 2.6	0.14
t <sub>1/2</sub> (hr)	14.3 $\pm$ 2.7	14.8 $\pm$ 3.2	0.25
Free fraction (%)	8.1 $\pm$ 0.7	8.4 $\pm$ 0.8	0.1

Data are mean values  $\pm$  SD.  
t<sub>max</sub>: Time to reach peak concentration.

Questions:

1. Provide a potential mechanistic explanation that could account for the observed effects, taking into consideration the large changes.
2. Describe how you would test your hypothesis using both *in vitro* and *in vivo* experiments.

The enzyme tyrosine hydroxylase (TH) plays an important role in the synthesis of multiple catecholamine neurotransmitters in the brain and periphery including dopamine (DA), norepinephrine (NE) and epinephrine (Epi). TH activity is well known to be enhanced by phosphorylation at multiple sites (e.g. Ser 8, Ser19, Ser31, Ser 40). TH Serine 40, in particular, has received significant attention as a major site of convergence of multiple protein kinases that can rapidly activate catecholamine production including PKA, PKG, p38MAPK and PKC isoforms. In recent studies of an adrenal chromaffin cell line (PC12), the PKC $\delta$ -specific inhibitor rottlerin (Figure 1), as well as treatment of cells with PKC $\delta$  RNAi, lead to an unexpected elevation of TH activity as measured by accumulation of L-dihydroxyphenylalanine (DOPA) using high-pressure liquid chromatography (HPLC) as well as increased phosphorylation at Ser30.

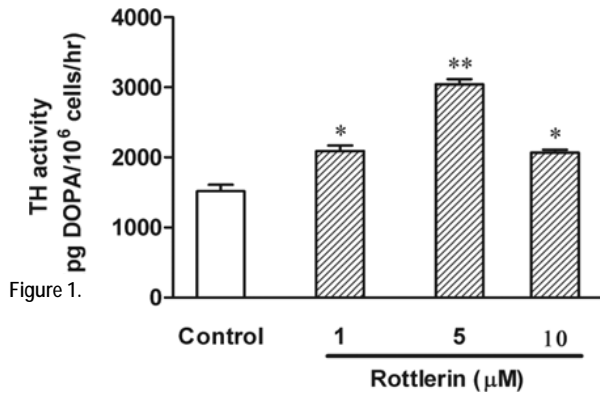
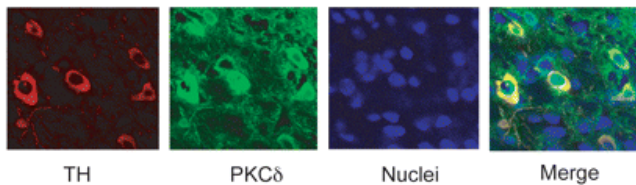


**Figure 1.** PKC $\delta$  inhibition enhances TH activity. PC12 cells were incubated with the DOPA decarboxylase inhibitor NSD-1015 (2 mM) for 1 h before treatment with the PKC $\delta$  inhibitor rottlerin (1–10 μM). DMSO (0.01%) was used as vehicle control. After 3 h of rottlerin treatment, cells were lysed and extracts were used for determining L-DOPA levels by HPLC. Rottlerin treatment increased L-DOPA levels, indicating enhanced TH activity. The data represent mean  $\pm$  SEM of six to eight individual measurements. Asterisks (\* $p$  < 0.05; \*\* $p$  < 0.01) indicate significant differences between rottlerin-treated cells and control cells.

Analysis of the cellular localization of PKC $\delta$  in CNS DA neurons in comparison with TH along with co-immunoprecipitation studies reveal the data provided in Figure 2. Finally, the Ser/Thr phosphatase PP2A specific inhibitor fostriecin reduces phosphorylation at S30 and decreases TH activity.

**A** Mouse Substantia nigra



**B** Mouse Substantia nigra



**C** PC12 cells

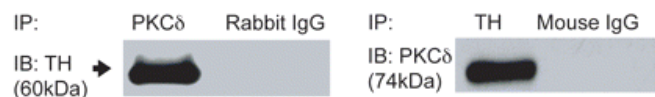


**Figure 2.** PKC $\delta$  associates with TH in mouse brain and PC12 cells. **A**, Immunohistochemical analysis. Mouse brain was cut to 20 μm thickness at the level of the substantia nigra and stained with PKC $\delta$  polyclonal antibody (Ab) (1:500 dilution) and TH monoclonal Ab (1:500 dilution), followed by incubation with either Alexa 488-conjugated (green; 1:1000) or Cy3-conjugated (red; 1:1000) secondary antibody. Hoechst 33342 (10 μg/ml) was used to stain the nucleus. Red, TH; green, PKC $\delta$ ; blue, nucleus. **B**, PKC $\delta$  (74 kDa) coimmunoprecipitated with TH in mouse substantia nigra. PKC $\delta$  was immunoprecipitated (IP) from mouse substantia nigra lysates by using PKC $\delta$  polyclonal Ab (1:100) and immunoblotted (IB) with anti-TH (1:100). In reverse immunoprecipitation studies, TH was immunoprecipitated with mouse monoclonal anti-TH antibody (1:100) and immunoblotted with PKC $\delta$ . TH (60 kDa) coimmunoprecipitated with PKC $\delta$  in mouse substantia nigra. Similarly, PKC $\delta$  (74 kDa) coimmunoprecipitated with TH in mouse substantia nigra. **C**, PKC $\delta$  also coimmunoprecipitated with TH in PC12 cells, and PKC $\delta$  was immunoprecipitated (IP) from PC12 cell lysates by using PKC $\delta$  polyclonal Ab (1:100) and immunoblotted (IB) with anti-TH (1:100). In reverse immunoprecipitation studies, TH was immunoprecipitated with mouse monoclonal anti-TH antibody (1:100) and immunoblotted with PKC $\delta$ . TH (60 kDa) coimmunoprecipitated with PKC $\delta$  in PC12 cell lysates. Similarly, PKC $\delta$  (74 kDa) coimmunoprecipitated with TH in PC12 cell lysates. Rabbit IgG and mouse IgG were used as negative controls.

A) Describe the steps that lead from amino acid precursor(s) to packaged catecholamine neurotransmitters, noting all major biosynthetic enzymes and transporters involved in the synthesis and storage of DA, NE and Epi. Describe the cell types and their location in the body that synthesize these catecholamines. Explain why the assessment of DOPA levels in PC12 cells pretreated with NSD-1015 is a suitable assay for TH activity.

Qualifying Exam – December 2007

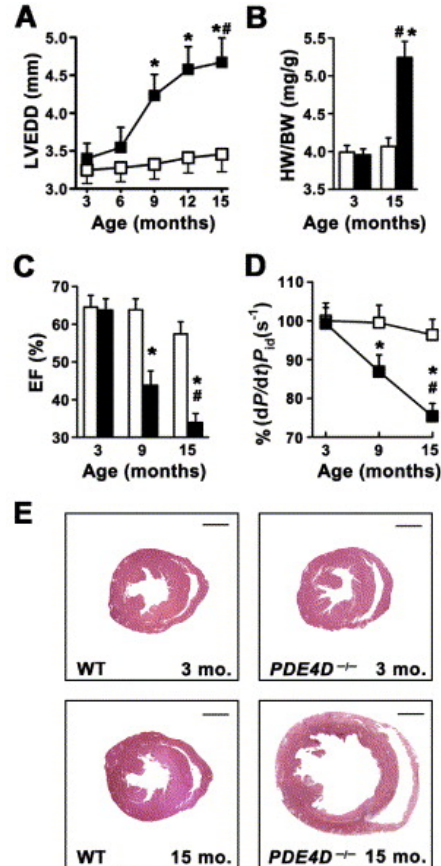
Question 4

B) Propose a model that is consistent with the data presented and which can explain how PKC $\delta$  can negatively regulate TH activity. Describe experiments that can be utilized to test critical aspects of your model and its suitability for TH regulation *in vitro* and *in vivo*.

C) Describe potential medical uses related to your model for PKC $\delta$  inhibitors and who you would not want taking these compounds.

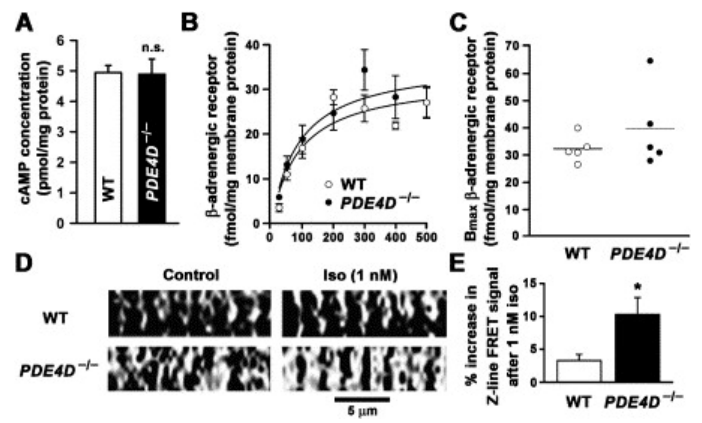
Targeted deletion of PDE4D in the mouse results in the cardiac phenotype presented in Figure 1. This is associated with normal global cAMP levels (Figure 2A,B) and beta adrenergic receptor levels (Figure 2C), but cAMP levels at the Z-lines are elevated (Figure 2D,E). PDE4D co-immunoprecipitates from human cardiac tissue with the ryanodine receptor (RyR2) (Figure 3A). In myocardium samples from patients with heart failure, PDE4D levels and activity are decreased while RyR2 phosphorylation is increased (Figure 3B,C). PDE4D activity coincident with RyR2 is confirmed by the use of a specific inhibitor (Figure 3D).

Figure 1



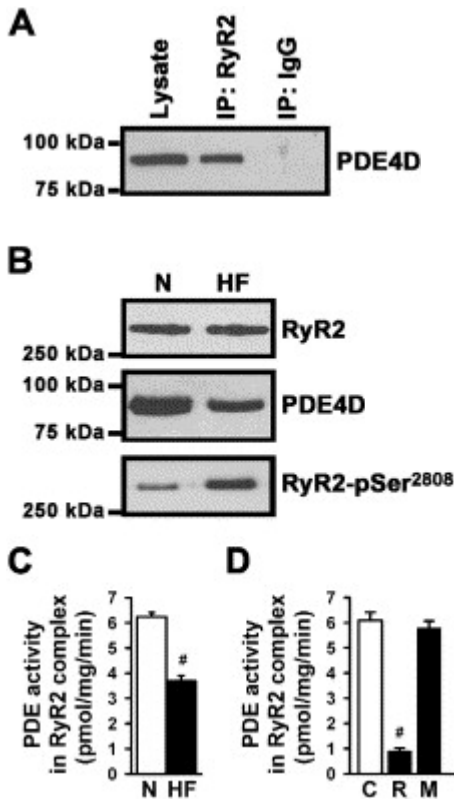
**Figure 1. PDE4D Deficiency Promotes Age-Related Cardiomyopathy** \*p < 0.05 versus wt; #p < 0.05 versus *PDE4D*<sup>-/-</sup>. (A) Echocardiography at 3 month intervals showing progressive increase in left ventricular end-diastolic diameter (LVEDD) in *PDE4D*<sup>-/-</sup> mice (open squares, wt; filled squares, *PDE4D*<sup>-/-</sup>; n = 12 each). Data in (A)–(D) are mean ± SEM. (B) Age-dependent increase in heart-to-body-weight ratio (HW/BW) in *PDE4D*<sup>-/-</sup> mice (open bar, wt; filled bar, *PDE4D*<sup>-/-</sup>). (C) Age-dependent decrease in ejection fraction (EF) in *PDE4D*<sup>-/-</sup> mice (open bar, wt; filled bar, *PDE4D*<sup>-/-</sup>). (D) Reduced cardiac contractility (dP/dt/P<sub>id</sub>) in *PDE4D*<sup>-/-</sup> mice at 3, 9, and 15 months of age (open squares, wt; filled squares, *PDE4D*<sup>-/-</sup>). (E) Histology showing dilated cardiomyopathy in PDE4D-deficient mouse hearts.

Figure 2



**Figure 2. Normal cAMP and β-Adrenergic-Receptor Levels in *PDE4D*<sup>-/-</sup> Mouse Hearts and Increased cAMP Levels at the Z Lines Detected by FRET-PKA** (A) cAMP concentrations were not significantly increased in hearts of 3- to 6-month-old *PDE4D*<sup>-/-</sup> mice (wt, n = 5; *PDE4D*<sup>-/-</sup>, n = 5; p = NS). Each heart was extracted and assayed separately in quadruplicate experiments. Data in (A), (B), and (E) are mean ± SD. (B) β-adrenergic-receptor density was unchanged in *PDE4D*<sup>-/-</sup> mice (wt, n = 5; *PDE4D*<sup>-/-</sup>, n = 5; p = NS). (C) Comparison of the B<sub>max</sub> values for β-adrenergic-receptor density calculated separately for each of the five wt or five *PDE4D*<sup>-/-</sup> knockout mice investigated. (D) FRET-PKA showing increased cAMP-dependent signal over the Z lines (site of localization of RyR2) after low-dose isoproterenol stimulation in *PDE4D*<sup>-/-</sup> cardiomyocyte when compared to wild-type cardiomyocyte (white and black areas represent sensing of highest and lowest cAMP concentrations, respectively). (E) Bar graph summarizes Z line intensity-profile analysis of 480 nm/545 nm intensity ratio from five wt and six *PDE4D*<sup>-/-</sup> cells (\*p < 0.05). Dimensions as indicated.

Figure 3



**Figure 3. Reduced PDE4D in the RyR2 Complex in Human Heart Failure** (A) PDE4D was detected in human cardiac lysate and in the immunoprecipitated RyR2 complex (IP:RyR2); IP:IgG, negative control. (B) RyR2 was immunoprecipitated from cardiac homogenates of normal human (N) and heart failure (HF) samples. PDE4D binding to RyR2 was significantly decreased in human HF. Increased PKA phosphorylation was detected by a phosphopeptide-specific RyR2-Ser2808 antibody in HF samples. (C) RyR2 bound PDE4D activity was significantly decreased in HF, as evidenced by close-proximity substrate cAMP catalysis ( $\#p < 0.001$ ). Data in (C) and (D) are mean  $\pm$  SD. (D) Rolipram (R), a PDE4-specific inhibitor, but not milrinone (M), a PDE3-specific inhibitor, decreased RyR2-associated PDE activity submaximally; C, control ( $\#p < 0.001$  versus untreated sample).

1. Describe the phenotype and outline how cAMP downstream of the Beta-adrenergic receptor regulates cardiac contractility.
2. State a hypothesis to describe the role of PDE4D in regulating RyR2 and heart function.
3. State a hypothesis as to how PDE4D and RYR2 are localized.
4. Several drugs that inhibit PDE's other than PDE4D are being developed for Alzheimer's disease therapy. Describe an *in vitro* screen for these compounds to exclude those with PDE4D inhibition.

A group of investigators studied the mechanisms mediating the effects of protease-activated receptor-2 (PAR2) on actin cytoskeleton. PAR2 is a G protein-coupled receptor. The authors focused on the filament-severing protein cofilin, which is activated in response to PAR2 stimulation by an agonist 2fAP. Activation of this protein requires its dephosphorylation at Ser-3 by cofilin-specific phosphatase chronofin (CIN). Below are the data they've obtained.

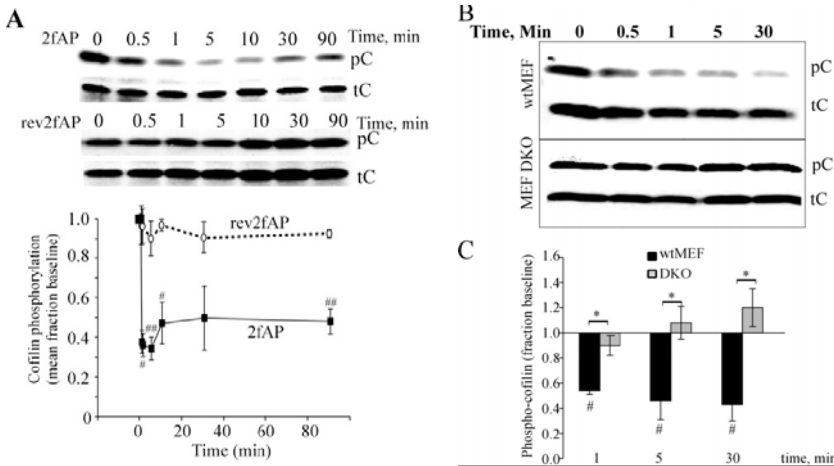


**Fig.1. A.** A time course (0-90 min) of cofilin activation after treatment with PAR2 agonist 2fAP or control inactive peptide with reversed sequence rev2fAP. Upper panel shown representative Western blot with phospho-Ser3-cofilin (pC) and total cofilin (tC) antibodies. Lower panel shows quantification of these data. **B.** Lysates of wild type (WT) mouse embryonic fibroblasts (MEFs) and MEFs where both beta-arrestin1 and beta-arrestin 2 were knocked out (double knockout or DKO) obtained at indicated times after PAR2 activation were subjected to Western blot using phospho-Ser3-cofilin (pC) and total cofilin (tC) antibodies. **C.** Quantification of the data shown in B. In both panels the statistical significance is shown, as follows: \*, p<0.05; #, p<0.01.

**Fig.2. Left panel (A).** Cofilin was immunoprecipitated after activation of PAR-2 with 2fAP and analyzed by SDSPAGE followed by Western blotting with anti-arrestin antibodies. All lanes contained the same amount of immunoprecipitated cofilin (not shown). **Right panel.** GFP-beta-arrestin-1 was co-expressed with or without FLAG-cofilin, after which cofilin was immunoprecipitated with anti-FLAG and analyzed by SDS-PAGE followed by Western blotting with anti-GFP (upper panel) or anti-cofilin (lower panel). *Cof*, cofilin; *TL*, total lysate;  $\beta$ 1 and  $\beta$ 2, beta-arrestin1 and 2.

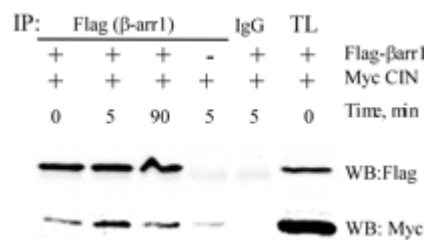
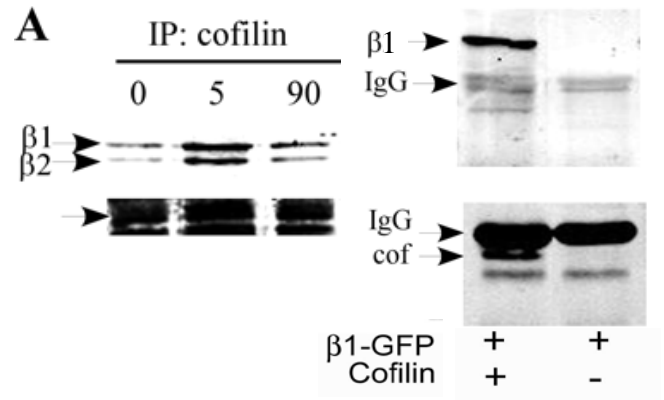


**Fig.3.** Cells were transfected with FLAG- beta-arrestin-1 and Myc-CIN or with Myc-CIN alone (lane 4) and treated with or without 2fAP. Cell extracts were immunoprecipitated with anti-FLAG (lanes 1–4) or IgG (lane 5) and Western blotted with anti-FLAG (upper panel) or anti-Myc (lower panel). Total lysate (TL) is shown in lane 6.

- Based on the findings presented in Figs.1-3, propose a molecular mechanism of PAR2-dependent cofilin activation.
- Propose experiments to test your model:
  - in cells that express endogenous PAR2;
  - in cells that do not express endogenous PAR2.
 Summarize the advantages and limitations of these two experimental models.
- You know that PAR2 couples to Gq. Propose experiments to test whether PAR2 signalling via Gq is involved in cofilin activation.

Mutations in the signaling pathway that control cell growth have been shown to underlie tumor initiation. Many of the key signaling components in this pathway include bioactive lipids. The growth factor receptor, Ras GTPase, PI(3) kinase and mTOR signaling pathway forms the core of a multi-intersecting network that drives cell growth based on environmental cues.

The chemotherapeutic drug Iressa (Gefitinib) has been shown to perturb this signaling pathway. In Table 1 the results from a lipid analysis are shown. Cells were dissociated from a solid tumor and grown in culture. The cells were labeled overnight with  $^3\text{H}$ -myo-inositol and separated using thin layer chromatography. The bands were scraped off the plate and quantitated in cpms. The indicated species were identified by relative migration of a synthetic standard. The cells were treated either with or without an  $\text{IC}_{50}$  dose of Iressa:

**Table 1**

<b>Tumor Cell-inositol lipid analysis</b>		
	<b>-</b>	<b>+ Iressa</b>
<b>C P M s</b>	PI	11,250
	PI4P	830
	PI(3,4)P <sub>2</sub>	340
	PI(4,5)P <sub>2</sub>	670
	PI(3,5)P <sub>2</sub>	480
	PI(3,4,5)P <sub>3</sub>	540
		13,340
		900
		120 *
		690
		200 *
		220 *

**Values are averages of 3 independent experiments with SEM < 5%. \* indicates statistical significant of  $p < .01$ .**

- (A) What is the molecular target of Iressa? Present a hypothesis that explains the effects on the inositol lipid content shown in Table 1 and subsequently effects mTOR activity. Design experiments to test this hypothesis and detail the parameters you would measure.